Eco-environmentally friendly operational regulation: An effective strategy to diminish the TDG supersaturation of reservoirs

Jingjie Feng, Ran Li, Ruifeng Liang and Xia Shen
State key laboratory of hydraulics and mountain river engineering, Sichuan University, No.24 of South Section One, Yihuang Road, Chengdu, 610065, China

Correspondence to: Ran Li (liran@scu.edu.cn)

Abstract: The presence of elevated total dissolved gas (TDG) downstream of a spillway may result in an increased incidence of gas bubble disease in fish. Supersaturated TDG is transported and dissipated more slowly in reservoirs than in natural rivers because of a higher water depth and lower turbulence and endangers fish. This paper presents the operational regulations concerning the mitigation of the TDG supersaturation impact on fish in the Bala Reservoir on the Zumuzu river. The paper includes the joint operations of the upstream and downstream power stations. A laterally averaged two-dimensional model is employed to simulate the TDG transportation and dissipation in the Bala Reservoir in addition to the hydrodynamics and water temperature. According to a comparison of the simulation results of different operational scenarios, this paper suggests a regulation scheme. With respect to the upstream power station, the adoption of an interval-discharge pattern instead of a continuous-discharge pattern is recommended to minimize the negative effect on the reservoir caused by supersaturated TDG. With respect to the downstream power station, the adoption of a surface tunnel rather than a bottom tunnel is recommended as a release structure. This paper is a reference for the eco-environmentally friendly operation of large and deep reservoirs.

1. Introduction

Involuntary spillage occurs in the high-runoff season. The phenomenon of TDG supersaturation is observed downstream of dam spill, which may lead to an increase in the incidence of gas bubble disease in fish (Weitkamp 1980, 2003). Levels of TDG saturation in excess of 130% have been observed downstream of many high-dam spills (Qu 2011). Supersaturated TDG always dissipates slowly in downstream flood transportation, and the dissipation may continue hundreds of kilometers downstream of the spillway. The dissipation rate depends on factors such as the water depth, turbulence, and temperature (Feng 2010). With the development of continuous cascade hydroelectric power systems, one deleterious impact on TDG transportation and dissipation is that the dissipation rate of TDG decreases substantially with an increase in water depth and a decrease in turbulence when a natural river is transformed into a reservoir. Consequently, the injury to fish is enhanced. The TDG transportation and distribution in a reservoir is closely related to the operation of upstream and downstream dams. To mitigate the detrimental effects to fish in the discharging period and to manage the conflict between the spill discharge and the aquatic system, operational regulation with respect to dam discharge is a viable strategy.

1.1 The previous studies

The development of hydroelectric power, especially with the development of continuous cascade systems, and the negative impacts of hydropower stations on the aquatic environment has attracted extensive attention. Recently, eco-environmentally friendly operational regulation has been investigated to assuage the conflict between hydropower development and

environmental protection. Yang (2013) has proposed an available operational method to decelerate the blooms in the tributary bays of the Three Gorges Reservoir. Lindim (2011) discussed the water quality changes in a large reservoir when water temperature is in stratification. An operational proposal is provided that minimizes the negative impact. Van Valit (2012) studied the effect of reservoir regulations on stream flow and thermal pollution on the Columbia River. Because climate changes and temperatures have increased in the Mekong basin in response to hydropower development, Lauri (2012) studied the optimization approach for multiple reservoir operations based on the hydrology analysis for the next 20 to 30 years. Nikoo (2013) developed an integrated water quantity-quality model for optimal water allocation in the reservoir-river basin that considered water supply and quality as targets in addition to hydrologic, water quality, and water demand uncertainties. To explore the impact on habitat suitability of carp in the Yangtze River following the construction of the Gezhouba and the Three Gorges Dams, a habitat suitability index model that considered the spawning characteristics of the four main carp species was established and employed by Yi (2010). Cai (2009, 2010) identified optimal strategies in the planning of energy and flood management aiming at fish protection and pursuing eco-environmentally friendly operations. Based on the calculated results, a minimum instream flow and suitable daily discharge increase during the reproduction season is suggested for the protection of the carp species. To balance human and ecosystem needs, Yin (2010) proposed a reservoir operation method that combines reservoir operating rule curves with the regulated minimum water release policy to meet the environmental flow requirements of riverine ecosystems. This operational method is applied to the Tanghe reservoir and Tanghe river basin. The prior research with respect to eco-environmentally friendly operations for reservoirs focuses on hydrology, sedimentation, water temperature and traditional water quality factors. The operational regulations for mitigating the negative impact of TDG, an important factor with respect to fish, are merely reported. According to the numerical results, Politano (2012) compared the TDG levels at the stilling basin downstream of Wells Dam under different configurations.

Dissolved oxygen (DO) was chosen as the main variable in the early studies on the negative impact on fish caused by dam spilling. Afterwards, TDG is studied as a new variable. According to the investigation of Ma (2013) , it's difficult to find a stable relationship between DO and TDG. In the authors' previous studies (Li, 2013), it was found that the TDG dissipation process is quantitatively different from the reaeration process of DO. Some biological studies also indicate that the supersaturated TDG is more harmful to the fishes than the supersaturated DO (Rucker, 1976). For these reasons, TDG is chosen as the key variable to study the eco-environmental regulations for mitigating the conflict between dam spilling and fish protect in the paper. The Enviromental Protection Agency of U.S. has recorgnized the threat to fish and has set water quality standards for dissolved gas level at 110% of saturation (U.S. EPA, 1986).

The prior studies reveal that the injury to fish is enhanced as the supersaturated TDG level and exposure time increases (Bentley, 1976; Huang, 2010; Chen, 2013). The endurance of fish with respect to supersaturated TDG is different depending on the growth period for the fish species (Liang, 2013).The impact of interval exposure to supersaturated TDG on fish was examined in a laboratory by Liu (2011). The results demonstrated that the damaged biological function of rock carp as a result of exposure to the TDG supersaturated water can recover when the rock carp is returned to fresh water. The research findings imply that the TDG impact on fish can be mitigated by reducing the exposure time and adjusting the manner of exposure of fish to TDG supersaturation.

The research findings suggest that optimized operational regulation of reservoirs is an effective approach to minimizing TDG levels in the reservoir and to the mitigation of the conflict between dam spilling and the protection of fish

1.2 Objective

This paper focuses on an operational strategy to minimize the negative effect of TDG in reservoirs. Numerical simulations are employed to compare the TDG distribution in Bala Reservoir under various configurations. An optimized regulation policy for Bala Reservoir is proposed based on the numerical results. Politano (2009), Urban (2008), and Fu (2011) have developed unsteady two-phase three dimensional models to calculate the TDG downstream evolution of spillways. The accuracy is satisfied in their simulations. However, these models are not applicable to large-scale bodies of water, such as reservoirs with a depth of more than 100 m and more than 100 km in length because they are limited by time cost and convergence. Therefore, this paper adopts a laterally averaged two-dimensional model that is proposed by the author (Feng, 2013) to predict the dynamics and the TDG levels in the simulations. The operational regulations of both the upstream and the downstream power stations are discussed.

2. The case study

Bala power station, with a maximum height of 138 m, is a high-dam hydropower station that is to be constructed on the Zumuzu River, source of the Daduhe River. The main discharge structures are a surface spillway tunnel and a bottom spillway tunnel. The elevation of the weir crest of the surface spillway tunnel is 2903 m and 2845 m for the bottom spillway tunnel. The backwater length of Bala Reservoir under normal water level is 26 km. At the upstream end of Bala Reservoir, a controlled cascade, Xiaerga Dam, is in the planning stages. The maximum height is 242 m. The main discharge structure is spillway. The dissipater of the spillway is designed as a ski-jump type model.

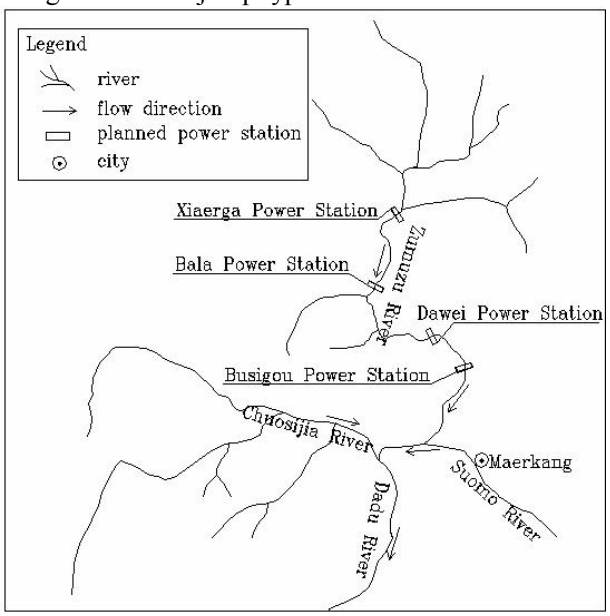

Fig. 1. The cascades on Zumuzu River

The fish species in the Zumuzu River is rare and endemic. The species include one type of Class Ⅱ nationally protected Chinese fish, *Hucho bleekeri*; two protected fish from the Sichuan Province, *Schizothorax (Racoma) davidi* and *Euchiloglanisdavidi*; and several endemic fish from the upper reaches of the Yangtze River, *Schizothorax (schizothorax.) prenanti* and

Sp. malacanthus chengi. The breeding periods of the rare and protected fishes in Zumuzu River are concentrated in April to July. Thus in the concentrated dam spilling period, the breeding and the growth of fish will be influenced.

The protection of the ecosystem during the hydropower development is a primary concern for the developers and scientists.

3. The methods and models

The TDG transportation and dissipation process is simulated in this study by employing the model developed by Feng (2013). This model is a two-dimensional laterally averaged hydrodynamic and water quality model. The hydrodynamics and the temperature are coupled-solved with the code CE-QUAL-W2. The simulation of the TDG transportation and dissipation is programed by the authors and incorporated into the CE-QUAL-W2 codes.

3.1 The governing equations

The governing equations of the model are listed as follows.

The continuity equation:

$$\frac{\partial UB}{\partial x}+\frac{\partial WB}{\partial z}=qB \tag{1}$$

The momentum equation:

$$\frac{\partial UB}{\partial t}+\frac{\partial UUB}{\partial x}+\frac{\partial WUB}{\partial z}=gB\sin\alpha-\frac{B}{\rho}\frac{\partial p}{\partial x}+\frac{1}{\rho}\frac{\partial B\tau_{xx}}{\partial x}+\frac{1}{\rho}\frac{\partial B\tau_{xz}}{\partial z} \tag{2}$$

$$\frac{1}{\rho}\frac{\partial p}{\partial z}=g\cos\alpha \tag{3}$$

The free water surface equation:

$$B_{\eta}\frac{\partial \eta}{\partial t}=\frac{\partial}{\partial x}\int_{\eta}^{h}UBdz-\int_{\eta}^{h}qBdz \tag{4}$$

The density is essential for the solution of the momentum equations. The equation of state relates the density to the temperature. The following relationship is used in the model

$$\rho=999.845259+6.793952\times10^{-2}T_w-9.19529\times10^{-3}T_w^{\ 2}+1.001685\times10^{-4}T_w^{\ 3}$$
$$-1.120083\times10^{-6}T_w^{\ 4}+6.536332\times10^{-9}T_w^{\ 5} \tag{5}$$

where U and W denote temporal mean velocity components in a horizontal and vertical direction; x and z represent the horizontal distance and vertical elevation; B is the width; q is the specific discharge; t denotes the time; g is the acceleration of gravity; p represents pressure and ρ denotes the density; τ_{xx} and τ_{xz} are defined as the turbulent shear stress acting in x direction on the x-face of control volume; α is the angle of the river bed to x direction; η and h are the water surface and water depth; T_w represent the water temperature. The universal transportation equation for scalar variables, such as temperature and TDG, is

$$\frac{\partial(\Phi B)}{\partial t}+\frac{\partial(UB\Phi)}{\partial x}+\frac{\partial(WB\Phi)}{\partial z}=\frac{\partial(BD_x)}{\partial x^2}+\frac{\partial(BD_z\Phi)}{\partial z^2}+S_{\Phi}B \tag{6}$$

where Φ denotes a scalar variable.

The source term for temperature consists only of surface heat exchange:

$$H_n=H_s+H_a+H_e+H_c-(H_{sr}+H_{ar}+H_{br}) \tag{7}$$

where H_n is the net rate of heat exchange across the water surface; H_s denotes the incident short wave solar radiation; H_a represents the incident long wave radiation; H_{sr} and

H_{ar} are the reflected radiations of short waves and long waves, respectively; H_{br} is the back radiation from the water surface; H_e represents the evaporative heat loss; and H_c denotes heat conduction.

The source term of TDG is defined as

$$S_\Phi = k_T(C_{eq} - C) + (K_L a)_s(C_s - C) \tag{8}$$

where C denotes the average TDG concentration expressed as a percent of the saturation concentration, C_s is the saturation concentration at local atmospheric pressure, C_{eq} is defined as the equilibrium saturation level of each cell relative to the local pressure and temperature, k_T is the dissipation coefficient of the water body and is zero when $C_{eq} - C > 0$, $(K_L a)_s$ is the surface mass transfer coefficient across the air-water surface interface and a denotes the specific surface area.

The following expression is widely used in the evaluation of the surface mass transfer coefficient across the air-water surface interface K_L:

$$K_L = 0.4Sc^{-1/2}(\nu\varepsilon)^{1/4} \tag{9}$$

where Sc is the Schmidt number $Sc = D/\nu$, D represents the molecular diffusion and ν denotes the eddy viscosity of water; ε is the rate of energy dissipation.

Because the rate of energy dissipation ε is not calculated in the model, another empirical formula to evaluate the surface mass transfer coefficient, $(K_L a)_s$, raised by O'Connor (1983), is employed in the model.

$$(K_L a)_s = -0.0045v_w{}^3 + 0.1535v_w{}^2 - 0.5026v_w + 0.6885 \tag{10}$$

where v_w represents the wind speed at a height of 10 m.

3.2 The discrete method

The finite difference method is implied in the discrete method of governing equations and transportation equation.

The discretization of the free water surface equation employs an explicit scheme. The discretization of the momentum equation employs a combining method, vertical diffusion is fully implicit and advection uses a time-weighted, central difference, implicit scheme. A unique feature of vertical advection, in the explicit part of the time-weighted scheme, is QUICKEST which increases the overall accuracy and is developed by Leonard. The discretization of the transportation equation uses a similar method as the momentum equation.

3.3 The model calibration and validation

Field observations were performed between July 26 and August 1, 2008, to study the TDG dissipation in the Dachaoshan Reservoir. Four transects were set along the reservoir to measure the TDG saturation of the water surface. A vertical line was planned at the 500 m upstream section of the Dachaoshan Dam. The TDG and depth data were collected at depth increments of approximately 5m.

The numerical model used in this study was employed by the author (Feng 2013) to simulate the unsteady dynamics and the TDG in the Dachaoshan Reservoir. The simulation results were consistent with the field measurements collected in this study, including the unsteady TDG saturation at each transect and the vertical distribution at the 500 m upstream section of the Dachaoshan Dam. The results demonstrated that the laterally averaged two-dimensional model is

applicable to the prediction of TDG transportation and dissipation in a reservoir.

The dissipation coefficient of 0.03 h^{-1} in the Dachaoshan Reservoir is numerically evaluated.

4. The simulation conditions

4.1 The case description and grid generation

P=5% (once-in-twenty-years) is taken as the flow condition at the dam site of Xiaerga, which is equal to 1910 m^3/s. The simulated period is 48 hours, from August 12 00:00 to August 13 24:00. The simulated region is 26 km long and stretches from the Xiaerga Dam to the Bala Dam. The topographic data of the Bala Reservoir are used to build the simulated zone. A structured mesh system, 500m in the longitudinal direction and 1m in the vertical direction, is generated. The grids of the simulation domain are shown in Figure 2.

Three scenarios are assumed for simulation according to the operational condition of Bala Reservoir in this paper. First, considering the effect of the discharging frequency, two scenarios are performed, Case 1 and Case 2. With respect to Case 1, 12 hour discharging is continuous. With respect to Case 2, the discharging time is equally divided into four time intervals, each lasting 3 hours. Second, to compare the effect of outlet elevation on the TDG distribution in the reservoir, Case 3 is set to contrast to Case 1. In Case 1, the flood runs out through the surface spilling tunnel of Bala at an elevation of 2903 m. In Case 3, the flood runs out through the bottom discharge tunnel at an elevation of 2845 m. The contrasts of the three cases are listed in Table 1.

Table 1. Case description and boundary conditions

Case No.	Upstream inflow					Downstream outflow		
	Discharge structure	Discharge pattern	Discharge flow rate (m^3/s)	Power flow (m^3/s)	TDG saturation level (%)	Discharge structure	Discharge pattern	Outlet elevation (m)
Case 1	Spillway	Continuous	1710	200	141	Surface spillway tunnel	Continuous	2903
Case 2	Spillway	Interval	1710	200	141	Surface spillway tunnel	Interval	2903
Case 3	Spillway	Continuous	1710	200	141	Bottom discharge tunnel	Continuous	2845

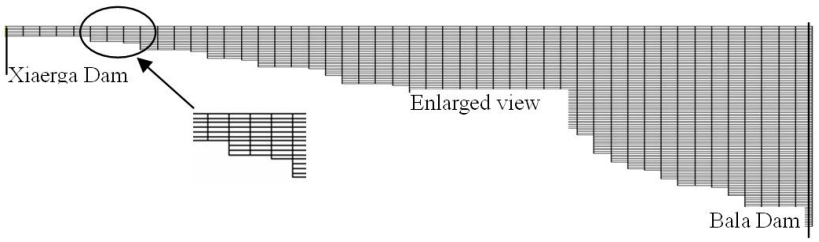

Fig. 2. Grid structure of Bala Reservoir

4.2 The initial conditions

The dynamics for this model are computed coupled with the temperature. The initial temperature field is significant to the formal simulation. The heat transfer from the air, the short wave solar radiation, the incident long wave radiation, the reflected radiations, and the evaporative heat loss are incorporated in the heat transport equation. By means of numerical simulation with a laterally averaged 2-D model, the initial temperature field is pre-computed by circularly calculating the dynamics and the water temperature month by month for two years. The

resulting temperature field for August is used as the initial field. During the pre-computation, the monthly hydrological data and inflow water temperatures are obtained from the Zumuzu hydrological station. The meteorological data are obtained from the Maerkang meteorological station. Fig. 3 presents the initial temperature field for the simulation.

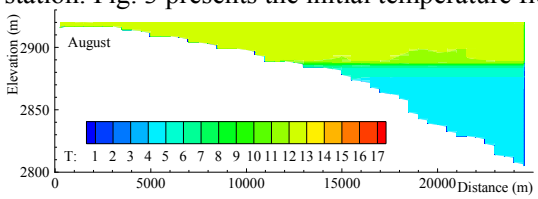

Fig. 3. The initial temperature field of Bala Reservoir (℃)

4.3 The boundary conditions

The TDG concentration and temperature of the inflow are based on field observation data. The boundary conditions versus time are presented in Fig. 4 and Fig. 5.

The power flow is 200 m^3/s and the upstream spillway discharge rate is 1710 m^3/s at the Xiaerga power station. Ignoring the daily regulation of Bala reservoir, the downstream outflow of Bala Reservoir is assumed to be the same as the upstream inflow and is presented in Fig. 4 and Fig. 5.

The TDG supersaturation level downstream of the Xiaerga spillway discharge is calculated with the empirical model proposed by Li (2009). The TDG supersaturation level of power flow is assumed to be the equilibrium saturation of tailrace, 100%. The flow-weighted average method is used to estimate the mixing TDG concentration of spill discharge and power flow. The flow weighted average TDG is calculated to be 141%. The inflow boundaries of TDG are presented in Fig. 4 and Fig. 5.

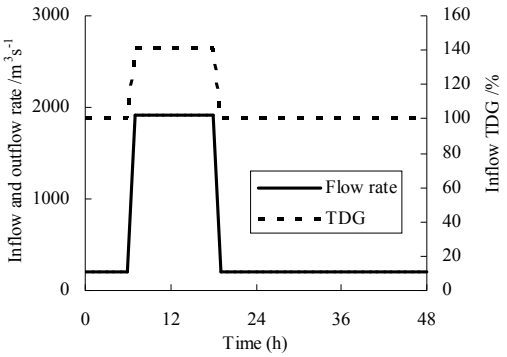

Fig. 4. The flow and TDG boundary conditions for Case 1 and Case 3

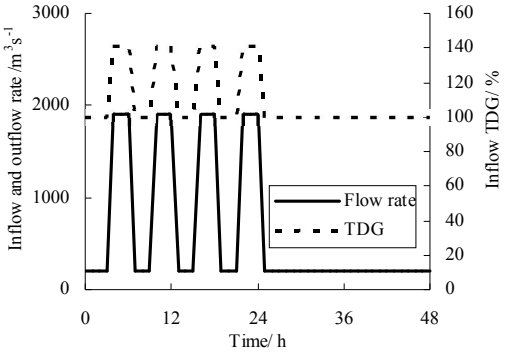

Fig. 5. The flow and TDG boundary conditions for Case 2

4.4 Parameter determination

The equilibrium saturation concentration C_{eq} varies with pressure, temperature and turbulence. In this simulation, the effect of hydrostatic pressure on the value of C_{eq} is considered as the following:

$$C_{eq}=100+10h \tag{11}$$

where h represents the local depth under the free surface.

The saturation concentration at local atmospheric pressure C_s is set at 100% in the simulation.

According to the parameter calibration in the Dachaoshan Reservoir, the dissipation coefficient, k_T, is determined to be 0.003 h^{-1} when the water is supersaturated,. Otherwise, k_T is assumed to be zero.

The surface mass transfer coefficient across the air-water free surface $(k_La)_s$ is calculated by Equation 10, where the wind speed is assumed to be 0.9 m/s according to meteorological data from the Maerkang weather station, 70 kilometers away from the Bala dam site.

5. Hydrodynamic and TDG Results of different operational regulations

5.1 Flow and temperature field

The predicted flow patterns in the Bala Reservoir are shown in Fig. 6 with streamlines colored by vector. The discrepancies in the three cases are mainly due to the outlet elevation. Case 1 and Case 2 have a similar stream line with a large circle backflow under the main current, which is in contrast to Case 3. With respect to case 3, the main current dives directly to the bottom at the point 7 km upstream of Bala Dam without obvious backflow in the field. A low velocity zone forms in the surface layers upstream of the dam. The maximum velocities of the three cases are approximately 3 m/s at the entrance of the reservoir. The velocity decreases further downstream because of the water depth increase. The velocity in the regions close to the Bala Dam is approximately 0.2 m/s for all three cases.

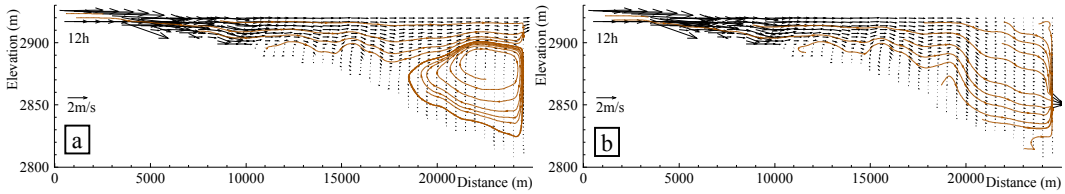

Fig. 6. Velocity vectors and streamlines in Bala Reservoir (a. Case 1 and Case 2; b. Case 3)

The initial temperature field (Fig. 3) demonstrates that the stratification of water temperature forms in Bala Reservoir in August. A 10 m-thick transition layer lies at a 30 m depth beneath the water surface. The temperature decrement between the two regions above and below the transition layer is as high as 8℃. When Xiaerga starts to spill, the initial stratification breaks because of the flood flow disturbance (Fig. 7a. After the spilling gates are closed, the reservoir water is gradually pacified and a new stratification forms again; this is presented in Fig. 7b. The flood significantly impacts the temperature stratification in the reservoir.

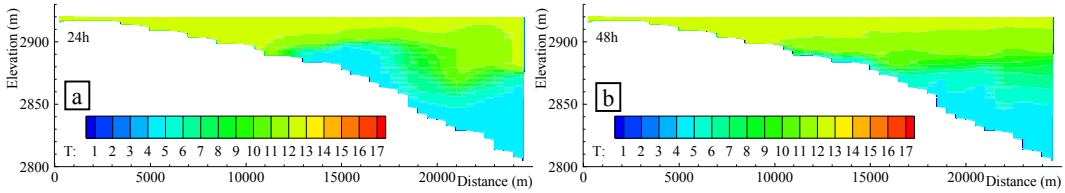

Fig. 7. Water temperature stratification in Bala Reservoir (℃)

5.2 TDG distribution

(1) Case 1 (continuous discharge + outflow through the high-elevation tunnel)

In Case 1, Xiaerga adopts a continuous discharge pattern as the inflow condition and the surface spilling tunnel is chosen as the outflow passageway. The TDG distributions in Bala Reservoir at different times are demonstrated in Fig. 8.

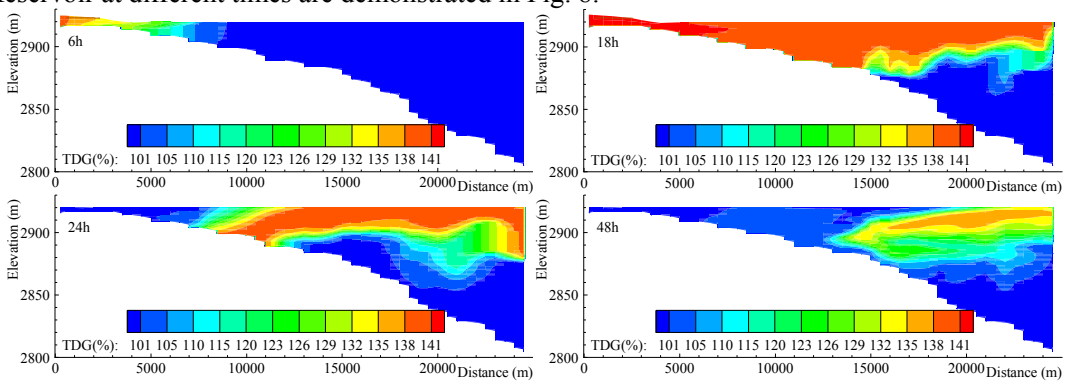

Fig. 8. The TDG distributions of Case 1 at different moment

ccording to Fig. 8, Xiaerga starts continuous flood discharge at the six-hour moment, continues for 12 hours and the generated TDG is 141% in saturation. The contours in Fig. 8 demonstrate that the supersaturated TDG appears in the entrance of Bala Reservoir at the six-hour moment. The transportation of TDG is in accordance with the main directional flow. A high TDG cluster is formed at the top layers of the reservoir. At the 18-hour moment, the effect of TDG supersaturation has already expanded to the dam with the flow current, with the maximum TDG saturation of 140.7%. In contrast to the inflow TDG saturation, 141%, the dissipation of

TDG is slight. This is because the flood discharge transports the elevated TDG flow at a high velocity. Therefore, the resident time for TDG flow in the reservoir is not long enough to complete the TDG degassing. After 18 hours, the flood discharge is shut and the inflow is composed only of the tailrace of Xiaerga with a TDG saturation of 100%. The supersaturated TDG flow then runs downstream of Bala at a slow pace and the degassing is sufficient because the resident time increases with the decreasing velocity. Consequently, the high TDG cluster becomes narrower and shorter over time. At the final moment of the simulation, the high TDG cluster is 10 km, with a maximum value of 136.2%.

(2) Case 2 (interrupted discharge and outflow through the high elevation tunnel)

In Case 2, Xiaerga adopts an interval discharge pattern as the inflow condition and the surface spilling tunnel is chosen as the outflow passageway. The TDG distributions in Bala Reservoir at different times are presented in Fig. 9.

At the three-hour moment, the spillway of Xiaer begins to work. The spillway gate is alternately opened and closed four times every 3 hours. Similar to Case 1, the high TDG clusters still appear at the top layers of Bala Reservoir as a result of the TDG transporting with the flow current. In contrast to Case 1, several clusters appear in the reservoir concurrently because of the interval flood discharge pattern. Fig. 9 demonstrates that at the 18-hour moment, four times the flood discharge brings the TDG cluster to the dam. At the 24-hour moment, the flood discharge is shut permanently in the simulation. The TDG in the reservoir then dissipates under the function of attenuation and sufficient degassing. At the end of the simulation, the negative region of TDG supersaturation is narrower than that of the prior moment, with a maximum TDG saturation of 135.3%.

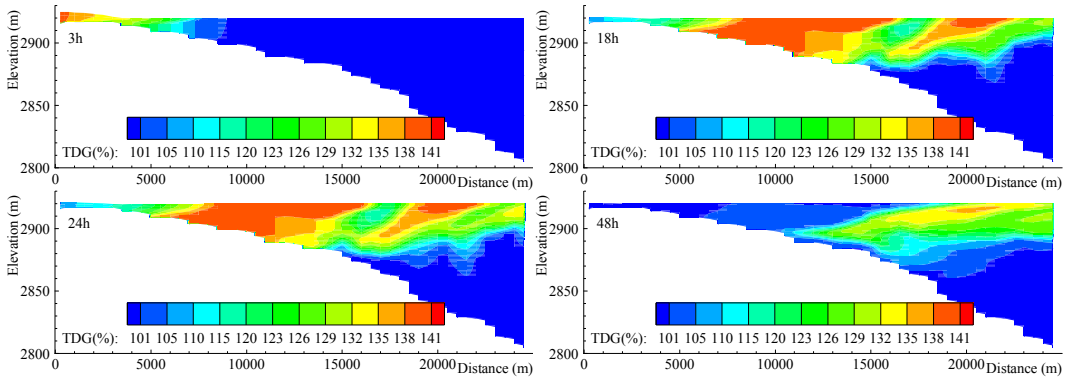

Fig. 9. The TDG distributions at different moments（Case 2）

(3) Case 3 (continuous discharge and outflow through the low elevation tunnel)

In Case 3, Xiaerga adopts a continuous discharge pattern as the inflow condition and the bottom discharge tunnel is chosen as the outflow passageway. The TDG distributions in Bala Reservoir at different moments are presented in Fig. 10.

At the six-hour moment, the continuous flood discharge begins and lasts for 12 hours. The high TDG cluster moves forward to the dam under high flood velocity without sufficient degassing for a long period. The TDG transport route is in accordance with the flow current streamline, therefore, the high TDG cluster spreads to the bottom as the bottom discharge tunnel is adopted as the flow passageway for Bala. The flood discharge is shut at 18 hours and approximately 80% of the reservoir is at a TDG level of 140% at that moment. The TDG level in the reservoir then decreases because of the attenuation and sufficient degassing with the extended resident time. A high TDG cluster lies at the bottom of the reservoir in accordance with the main current. At the final moment of the simulation, the negative region of TDG supersaturation is

narrower with a maximum TDG saturation of 136.8%.

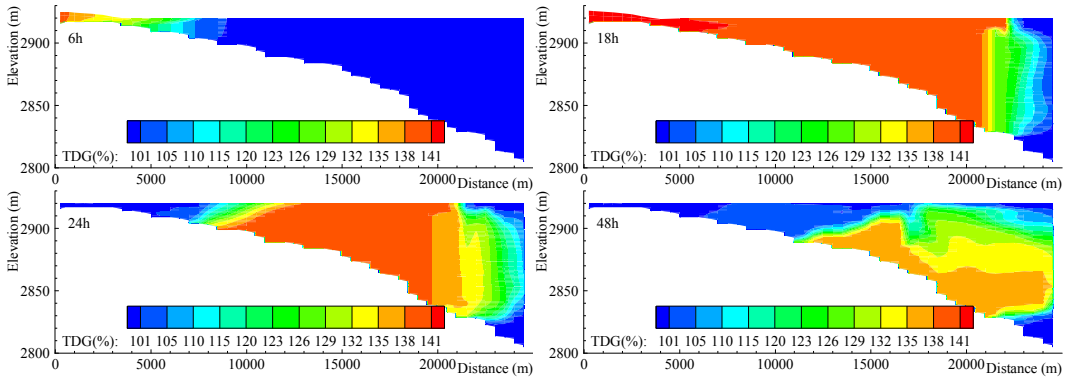

Fig. 10. The TDG distributions at the key moments（Case 3）

6. Discussions on the effect of operational regulations

The TDG results indicate that different inflow boundary conditions result in different distributions of TDG in Bala Reservoir. This study analyzes regulation effects from two aspects, the operation of the upstream power station (inflow condition) and the operation of the downstream power station (outflow condition).

6.1 Regulation of the upstream power station

Case 1 and Case 2 adopted two different inflow boundary conditions -- the continuous discharge pattern and the interval discharge pattern of the upstream Xierga Dam (Fig. 4). A comparison between Case 1 and Case 2 demonstrates the effect of the regulations of Xiaerga power station, the upstream power station.

Fig. 11 presents the TDG comparison of the two cases at the moment when the discharge time accumulates to 12 hours. It demonstrates that a high TDG cluster with a thickness of 25 m is formed at the surface of Bala Reservoir in Case 1 with a maximum TDG saturation of over 138%. Several high TDG clusters are formed in Case 2 that are caused by the interval flood discharge pattern. The high-TDG area in Case 2 is significantly smaller than that of Case 1.

A comparison of the two cases at the moment when the off-time of the spillway tunnel accumulates to 24 hours is presented in Fig. 12. The contrast demonstrates that the TDG levels are significantly less than at the same moment in Fig. 11. For both cases, the high TDG clusters are distributed around the surface layers in the 13 km range in the front of Bala Dam.

To quantitatively compare the supersaturated TDG effect of the two cases, accumulative curves of area ratio are drawn in Fig. 13. The horizontal coordinate represents the TDG percent saturation. The vertical coordinate is defined as the area ratio of the TDG saturation area that is higher than the corresponding saturation for the whole reservoir. At the moment when the flood discharge time accumulates to 12 hours, the area ratio percent of Case 2 is much lower than Case 1. When the off-time accumulates to 24 hours, the area ratio percent of the two cases is proximal, with the exception of TDG, which ranges from 130% to 135%.

To minimize the TDG supersaturation in a reservoir, the comparison of Case 1 and Case 2 demonstrate that an upstream interval-discharge pattern is more effective than a continuous flood discharge pattern.

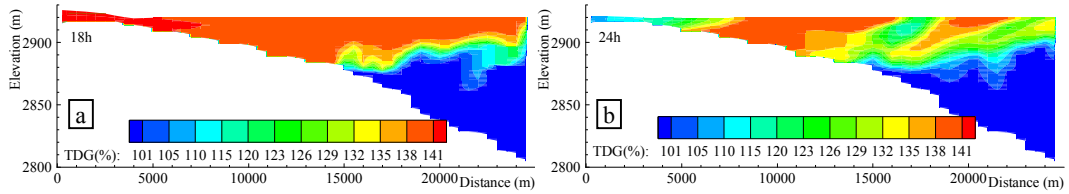

Fig. 11. Comparison of TDG distributions at the moment of accumulated flood discharge time of 12 hours (a. Case 1; b. Case 2)

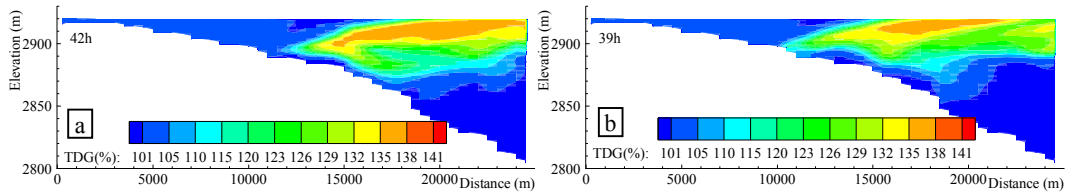

Fig. 12. Comparison of TDG distributions at the moment of accumulated off-time of 24 hours (a. Case 1; b. Case 2)

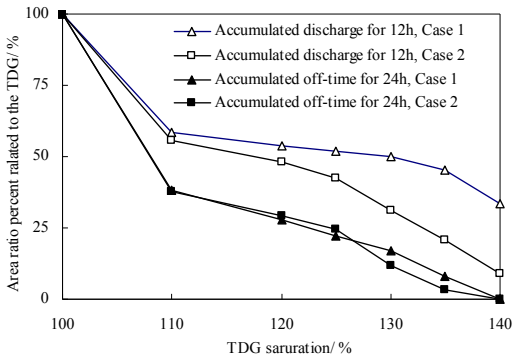

Fig. 13. Accumulated curves of area ratio percent

6.2 Regulation of downstream power stations

Case 1 and Case 3 adopt different release structures of the downstream Bala Dam, which are operated with different elevations. The surface spillway tunnel at 2903 m is chosen in Case 1 and the bottom discharge tunnel at 2845 m is chosen for Case 3. The inflow boundaries are the same for the two cases. The comparison between Case 1 and Case 3 demonstrate the effect of operational regulations on the Bala power station, the downstream power station.

Fig. 14 presents the TDG comparison of the two cases at the moment when the discharge time accumulates to 12 hours. It demonstrates that a high TDG cluster with a thickness of 25 m is formed at the surface of Bala Reservoir in Case 1. In Case 3, the supersaturated TDG spread from the surface to the bottom as the surface streamlines turns towards the bottom. The high-TDG area in Case 3 is significantly larger than that of Case 1.

Another comparison of the two cases is analyzed at the moment when the off-time of the spillway tunnel accumulates to 24 hours and is presented in Fig. 15. The contrast demonstrates that the TDG levels are significantly decreased than at the time in Fig. 14. In Case 1, the high TDG cluster is distributed around the surface layers in the 13 km range in front of Bala Dam. In Case 3, the high TDG cluster is distributed at the bottom 15 km range at the front of the dam.

To minimize the TDG supersaturation in a reservoir, the comparison of Case 1 and Case 3

demonstrate that a downstream surface-discharge pattern is more effective than a bottom-discharge pattern.

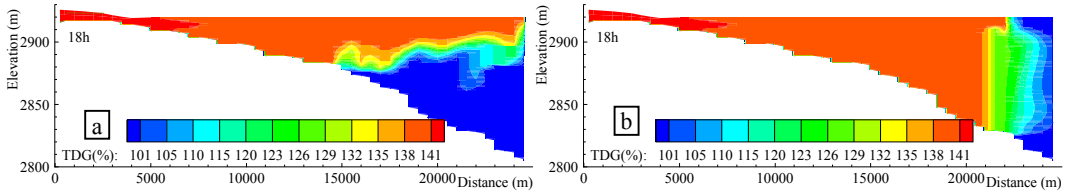

Fig. 14. Comparison of TDG distribution of Case 1(a) and Case 3(b) at the moment of accumulative discharge time of 12 hours

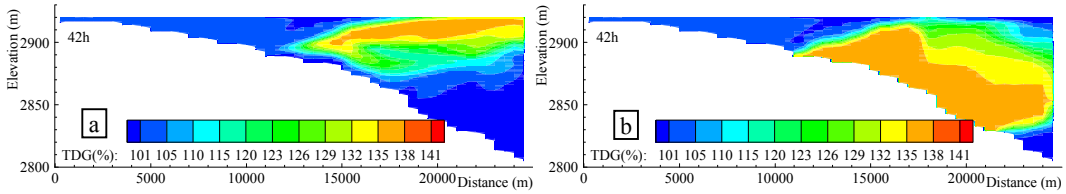

Fig. 15. Comparison of TDG distribution of Case 1(a) and Case 3(b) at the moment of accumulated off-time of 24 hours

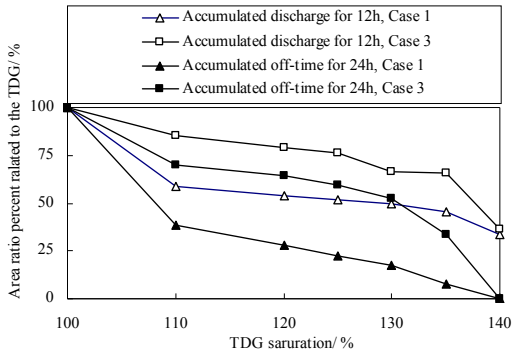

Fig. 16. Accumulated area ratio over TDG saturation level

7. Conclusions

The regulation of operations is an effective way to mitigate the harmful TDG supersaturation in the Bala Reservoir on the Zumuzu River. This paper employed a laterally averaged two-dimensional model to simulate the TDG distributions of different spill scenarios, including the configuration combinations of the upstream and downstream power stations.

The results indicate that the TDG distribution is mainly affected by the movement of the current flow. When a spillway is discharged, the supersaturated TDG moves rapidly towards the Bala Dam with the main current. Small amounts of dissipation happen in such a deep reservoir. The TDG saturation level remains high until it reaches the downstream Bala Dam at a maximum TDG level that is higher than 138%. The protection of aquatic organisms in the large reservoirs during the discharging period is a concern.

According to the comparison of the scenario simulation results, the optimized regulations for the reservoir are concluded. For the upstream power station, an interval-discharge pattern instead of a continuous-discharge pattern is recommended to minimize the negative effect in the

reservoir that is caused by supersaturated TDG. For the downstream power station, the use of a surface tunnel rather than a bottom tunnel is recommended as a release structure.

Future modeling efforts are suggested to combine the endurance of fish with respect to supersaturated TDG and to propose mitigation measures. The effect of the regulation on the downstream river is also another important and sophisticate problem that needs to be addressed respectively in the future.

Acknowledgements. This material is based upon work supported by the National Natural Science Foundation of China, Grant No. 51179111.

References

Bentley, W.W., Dawley, E.M., Newcomb, T.W.: Some effects of excess dissolved gas on squawfish, Ptychocheilus oregonensis (Richardson). Technical Information Center; Oak Ridge, Tennessee. 41-46, 1976

Cai, Y.P., Huang, G.H., Yang, Z.F., Tan, Q.: Identification of optimal strategies for energy management systems planning under multiple uncertainties. Applied Energy, 86, 480-495, 2009.

Cai, Y.P., Huang, G.H., Tan, Q., Chen, B.: Identification of optimal strategies for improving eco-resilience to floods in ecologically vulnerable regions of a wetland. Ecological Modelling, 222, 360-369, 2010.

Chen, S.C., Liu, X.Q., Jiang, W., et al.: Effects of total dissolved gas supersaturated water on lethality and catalase activity of Chinese Sucker (Myxocyprinus asiaticus Bleeker), Journal of Zhejiang University-SCIENCE B (Biomedicine & Biotechnology), 13, 791-796, 2012.

Feng, J.J, Li, R., Li, K.F., et al: Study on release process of supersaturated total dissolved gas downstream of high dam. Journal of Hydroelectric Engineering, 29, 7-12, 2010. (In Chinese)

Feng, J.J., Li, R., Yang, H.X., Li, J.: A laterally averaged two-dimensional simulation of unsteady supersaturated total dissolved gas in deep reservoir, Journal of Hydrodynamics, 25, 396-403, 2013.

Fu, X.L., Li, D., Zhang, X.F.: Simulations of the three-dimensional total dissolved gas saturation downstream of spillways under unsteady conditions, Journal of Hydrodynamics, 22, 598-604, 2010.

Huang, X., Li, K.F., Du, J., Li, R.: Effects of gas supersaturation on lethality and avoidance responses in juvenile rock carp (Procypris rabaudi Tchang), Journal of Zhejiang University-SCIENCE B (Biomedicine & Biotechnology), 11, 806-811, 2010.

Lauri, H., de Moel, H., Ward, P.J. et al.: Future changes in Mekong River hydrology: impact of climate change and reservoir operation on discharge, Hydrol. Earth Syst. Sc., 16, 4603-4619, 2012.

Li, R., Li, J., Li K.F., et al.: Prediction for supersaturated total dissolved gas in high-dam hydropower projects, Science in China, Series E: Technological Sciences, 52, 3661-3667, 2009.

Li, R., Hodges, B.R., Feng, J.J., Yong, X.D.: A comparison of supersaturated total dissolved gas dissipation with dissolved oxygen dissipation and reaeration, Journal of Environmental Engineering, ASCE, 139, 385-390, 2013.

Liang, R.F., Li, B., Li, K.F., Tuo Y.C.: Effect of total dissolved gas supersaturated water on early life of David's schizothoracin (Schizothorax davidi), Journal of Zhejiang University-SCIENCE B (Biomedicine & Biotechnology), 14, 632-639, 2013.

Lindim, C., Pinho, J.L., Vieira, J.M.P.: Analysis of spatial and temporal patterns in a large reservoir using water quality and hydrodynamic modeling, Ecological Modelling, 222, 2485-2494, 2011.

Liu, X.Q., Li, K.F., Du, J.,et al.: Growth rate, catalase and superoxide dismutas activities in rock carp (Procypris rabaudi Tchang) exposed to supersaturated total dissolved gas, Journal of Zhejiang University-SCIENCE B (Biomedicine & Biotechnology), 12, 909-914, 2011.

Ma, Q., Li, R., Feng, J.J., Wang, L.L.: Relationships between total dissolved gas and dissolved oxygen in water, Fresenius Environmental Bulletin, 22, 3243-3250, 2013.

Nikoo, M.R., Karimi, A., Kerachian, R.: Optimal Long-term Operation of Reservoir-river Systems under Hydrologic Uncertainties: Application of Interval Programming, Water Resource Management, 27, 3865-3883, 2013.

O'Connor D: Wind effects on gas-liquid transfer coefficients, J. Environ. Eng.-ASCE, 109, 731-752, 1983.

Politano, M., Amado, A.A., Bickford, S. et al.: Evaluation of operational strategies to minimize gas supersaturation downstream of a dam, Comput. Fluids, 68, 168-185, 2012.

Qu, L., Li, R., Li, J., et al.: Field observation of total dissolved gas supersaturation of high-dams, Science in China, Series E: Technological Sciences, 54, 156-162, 2011.

Rucker, R.R.: Gas-bubble disease: Moralities of coho salmon, Oncorhynchus kisutch, in water with constant total gas pressure and different oxygen-nitrogen ratio, Fish Bull, 73, 915-918, 1976.
Urban, A.L., Gulliver, J.S., Johnson, D.W.: Modeling total dissolved gas concentration downstream of spillways, J. Hydraul. Eng.-ASCE, 134, 550-561, 2008.
Van Vliet, M.T.H., Yearsley, J.R., Franssen, W.H.P. et al.: Coupled daily stream flow and water temperature modelling in large river basins, Hydrol. Earth Syst. Sc., 16, 4303-4321, 2012.
Weitkamp, D.E., Sullivan, R.D., Swant, T., et al. Gas bubble disease in resident fish of the lower Clark Fork River, Trans. of the Am. Fisheries Soc., 132, 865-876, 2003.
Yang, Z.J., Liu, D.F., Ji, D.B.: An eco-environmental friendly operation: An effective method to mitigate the harmful blooms in the tributary bays of Three Gorges Reservoir, Science China- Technological Sciences, 56, 1458-1470, 2013.
Yi, Y.J., Wang, Z.Y., Yang, Z.F.: Impact of the Gezhouba and Three Gorges Dams on habitat suitability of carps in the Yangtze River, Journal of Hydrology, 387, 283-291, 2010.
Yin, X., Yang, Z.F., Yang, W., et al.: Optimized reservoir operation to balance human and riverine ecosystem needs: model development, and a case study for the Tanghe reservoir, Tang river basin, China, Hydrological Processes, 24, 461-471, 2010.